Application of SIMSTEX to Oligomerization of Insulin Analogs and Mutants

Raghu K. Chitta, Don L. Rempel, Michael A. Grayson, Edward E. Remsen, and Michael L. Gross
Department of Chemistry, Washington University, St. Louis, Missouri, USA

The propensity of various insulins and their analogs to oligomerize was investigated by mass spectrometric methods including measurement of the relative abundances of oligomers in the gas phase and the kinetics of H/D amide exchange. The kinetics of deuterium uptake show a good fit when the exchanging amides are placed in three kinetic groups: fast, intermediate, and slow. r-Human insulin, of the insulins investigated, has fewer amides that exchange at intermediate rates and more that exchange at slow rates, in accord with its higher extent of association in solution. We adapted PLIMSTEX (protein ligand interactions by mass spectrometry, titration, and H/D exchange) to determine protein/ligand affinities in solution, to determine self-association equilibrium constants for proteins, and to apply them to various insulin analogs. We term this adaptation SIMSTEX (self-association interactions using mass spectrometry, self-titration and H/D exchange); it gives affinity constants that compare well with the literature results. The results from SIMSTEX show that some mutants (e.g., GlnB13) have an increased tendency to self-associate, possibly slowing down their action in vivo. Other mutants (e.g., lispro and AspB9) have lower propensities for self-association, thus providing potentially faster-acting analogs for use in controlling diabetes. (J Am Soc Mass Spectrom 2006, 17, 1526–1534) © 2006 American Society for Mass Spectrometry

Insulin, a protein with 51 amino acid residues in two chains, which are linked together by two disulfide bonds and is produced in the pancreas to regulate blood glucose levels (Scheme **1**), self-associates in solution [1, 2]. It is stored in the pancreas as a hexamer, but the active form is a monomer [1, 2]. The hexamer must dissociate into monomers for absorption into the blood stream. An issue for r-human insulin and for any analogs to be used in the treatment of diabetes is the role of its structural form on the onset time and duration of action. One hypothesis is that the higher the tendency of an insulin to self-associate, the longer it takes to act [3].

In type 1 diabetes, insulin-producing cells are destroyed, and blood glucose levels must be controlled by injection of r-human insulin or its analogs. Strict control of blood glucose levels is difficult because conventional delivery methods do not mimic the quick physiological release from the pancreas in response to the increased glucose levels that follow a meal, for example [4]. r-Human insulin has an onset time of ~30 min, and 5 to 12 h of action [2, 4] and, therefore, one must administer it 30 to 60 min before meals to achieve optimal control of glucose levels [3, 5]. One reason for long onset for r-human insulin is that the hexameric form must dissociate to the monomeric form [2]; thus, insulin mutants that readily dissociate into monomers should be faster-acting [3, 5]. The effect of such mutations on oligomerization also provides insight into intermolecular interactions and points the way to the design of new insulin analogs that are fast- or prolonged-acting [3, 6, 7]. Some mutants, in fact, are reasonably well-understood and are currently used in the treatment of diabetes [7, 8].

One FDA-approved analog of insulin is "lispro" [9], a protein in which the amino acids in positions B28 (proline) and B29 (lysine) of the B-chain of human insulin are exchanged. This simple switch causes a decrease in the dimerization constant, leading to enhanced dissociation owing to the loss of key hydrophobic interactions in lispro compared with human insulin [2, 9]. The orientation of Pro in the B-chain is towards the dimer interface in human insulin (Scheme **2**), whereas it is facing away from the interface in lispro (Scheme **3**). The observation that most of the interactions involved in dimerization occur in the C-terminal region of the B-chain (except for Asp^{A21}) [10, 11] may explain this significant effect on the oligomerization tendency. The binding of lispro to the insulin receptor and its immunogenicity [3, 9] are, however, not affected by the mutations.

X-ray crystallography [10, 11] shows that dimer formation occurs mainly by nonpolar interactions involving B23-B26 and B28 in the C-terminal region of the

Published online September 6, 2006
Address reprint requests to Dr. M. L. Gross, Department of Chemistry, Box 1134, Washington University, One Brookings Drive, St. Louis, MO 63130, USA. E-mail: mgross@wustl.edu

1044-0305/06/$32.00
doi:10.1016/j.jasms.2006.08.004

Received April 10, 2006
Revised August 4, 2006
Accepted August 4, 2006

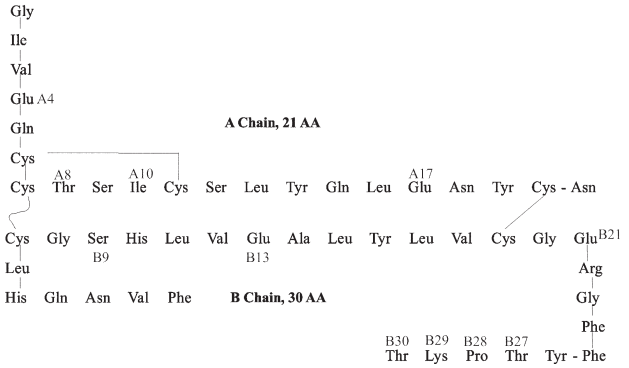

Scheme 1. The sequence of human insulin. Insulin consists of two chains, A and B, having 21 and 30 amino acids, respectively. The amino acids that are changed to obtain various insulin mutants (the mutations are shown in Tables 1 and 2) are labeled with the chain name, followed by the amino acid number in the chain.

B chain and by hydrogen bonding involving residues B24 and B26 [11]. In the A-chain, Asn^{A21} seems to be the only amino acid that is involved in dimer formation. More evidence of the importance of the B chain interface in wild-type insulin (shown in Scheme **2**) comes from the observation that insulin mutants without B26-B30 and B28-B30 regions do not dimerize [12]. Formation of hexamers occurs by burial of both polar and nonpolar residues between the dimers leading to looser packing than that of the dimer [2, 11, 13]. Six Glu^{B13} are arranged in a circular pattern at the center of the hexamer, with charge repulsion counteracted by Zn-binding [3]. When Glu^{B13} is changed to Gln, a slow-acting insulin results [13] owing to a reduction of charge repulsion and an increase in hexamerization.

Our hypothesis is that mass spectrometry combined with H/D amide exchange and mathematical modeling can reveal the effects of mutations on the oligomerization properties of proteins, and specifically on various insulins. We report here a mass spectrometric method to determine the self-association properties of proteins, and we apply the method to insulin. We also wish to

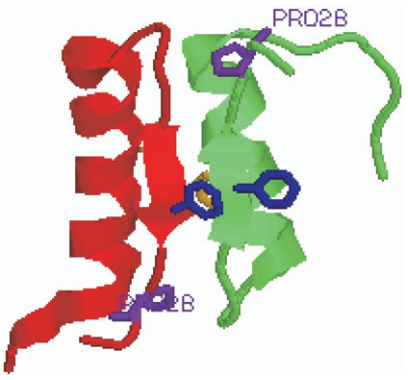

Scheme 2. The dimer interface for the human insulin. A stronger, more compact dimer results because orientation of Pro^{B28} is towards the interface forming a hydrophobic contact. Coordinates were taken from RCSB Protein Data Bank, file 1ZNI.pdb.

Scheme 3. The dimer interface for the lispro dimer. An important hydrophobic contact in the dimer is eliminated because the Pro^{B29} is away from the interface. Coordinates were taken from RCSB Protein Data Bank, file 1LPH.pdb.

resolve issues with solubility of insulin in the earlier kinetic results reported in [14], a report in which the kinetics of amide exchange was used without modeling to distinguish various forms of insulin. We now fit the data for r-human, lispro, porcine, and bovine insulins, whose sequences are shown in Table 1, to a kinetic model similar to the one used in [15]. Exchange reactions for proteins and peptides were successfully modeled as pseudo first-order reactions [16], and three exchange rate grouping models were previously applied to the kinetics of exchange of other proteins [15].

H/D amide exchange is useful for studying the higher order structure of proteins in solution [17, 18]. Its use in mapping protein/protein interfaces was pioneered by Komives and coworkers [19, 20]. The premise for their strategy is that amides buried in an interface will exchange more slowly in the complex than when the protein is free and not part of a complex. H/D exchange can also provide thermodynamic information about protein/ligand binding [21]. Two H/D exchange methods, SUPREX [21] and PLIMSTEX [22], make use of H/D exchange in a titration format to obtain the free-energy and affinity for the binding. To adapt PLIMSTEX to self-association requires the mathematical modeling of PLIMSTEX to be changed (no modifications are required for SUPREX). In this paper, we describe those modifications and apply the modified method, which we call SIMSTEX (self interactions by mass spectrometry self-titration and H/D exchange) to

Table 1. Sequence variations for insulin analogs studied here compared to human insulin

Insulin type	Sequence variation
Lispro	K^{B28} and P^{B29} reversed
Bovine	A in B30
Porcine	A in B30, A in A8 and V in A10

Table 2. Insulin mutants studied in this work

Insulin mutant	Mutation
A4A17	Glu^{A4} and Glu^{A17} to Gln and Tyr^{B31}
B27	Thr^{B27} to Arg
A4B27	Glu^{A4} to Gln and Thr^{B27} to Arg
B9Asp	Ser^{B9} to Asp
B21	Glu^{B21} to Gln
B13B21	Glu^{B13} and Glu^{B21} to Gln

r-human insulin and to various insulin analogs to obtain affinity constants for self-association. The various insulins were designed by others to increase or decrease hexamerization [2, 3] as can be seen by considering the interface between two insulin molecules in the dimer in Scheme **2**.

Methods

Materials

r-Human Insulin was purchased from Sigma (Milwaukee, WI). Porcine, bovine, and lispro insulins were gifts from the Food and Drug Administration of St. Louis. Other insulin mutants were donated by Dr. Stephen Bayne of NovoNordisk, Denmark, and were formed by mutating one or two residues at a time of human insulin [the list of mutants, their names (as used in this article), and the corresponding mutation(s) are shown in Table 2]. All the insulin analogs were dissolved in 10-mM ammonium acetate at pH 2.5. The pH was then raised to 7.4 by slowly adding ammonia. The solution was then centrifuged, and the supernatant supersaturated solution was taken for study.

To obtain an independent assessment of the oligomerization state of insulin in solution, hydrodynamic diameter distributions for the protein solutions were determined by dynamic light scattering (DLS) under both pH conditions. A Brookhaven Instruments Co. (Holtsville, NY) DLS system consisting of a model BI-200SM goniometer, a model EMI-9865 photomultiplier, and a model 95-2 Ar ion laser (Lexel Corp., Palo Alto, CA) operated at 514.5 nm was employed. All measurements were made at 20 ± 1 °C. Before analysis, insulin solutions were centrifuged for 4 min at 8000 × *g* in a Brinkman model 5415 microfuge to sediment any extraneous particles. Scattered light was collected at a scattering angle 90°. The system's digital correlator was operated with 522 channels, ratio channel spacing, initial and final delay settings between 1.4 μs and 10 ms, respectively, and duration of 10 min. A photomultiplier aperture of 200 or 400 μm was used, and the incident laser intensity was adjusted to obtain a photon counting rate of 200 to 300 kcps. Only measurements for which the measured and calculated intensity autocorrelation function agreed to within 0.1% were used to calculate hydrodynamic diameters. Calculations of the hydrodynamic diameter distribution from measured intensity autocorrelation functions were performed with the ISDA software package (Brookhaven Instruments Co., Holtsville, NY), which employed single exponential fitting, cumulant analysis, and non-negatively constrained least-squares (NNLS), and continuous regularization (CONTIN) analysis routines. Reported hydrodynamic diameter distribution averages are mean values of a minimum of three determinations.

For amide H/D exchange studies, the insulin in ammonium acetate was diluted 10-fold in deuterated ammonium acetate. For kinetics measurements, the uptake of deuterium was monitored as a function of the time for quenching the reaction in ice-cold water/acetonitrile/formic acid 50/49/1. To follow the deuterium uptake as a function of concentration, the H/D exchange was allowed to reach steady-state (~6 h). The exchange was quenched, and the solution at a final insulin concentration of 10 μM was infused into the ESI source for MS measurement. The quench caused the oligomers to dissociate into monomers. The deuterium uptake was measured as the difference between the mass centroids of the monomer distribution after and before exchange.

Mass Spectrometry

Mass spectra of the dimer in various solvents were acquired with a Q-TOf-*Ultima* (Micromass, Manchester, UK), a tandem mass spectrometer consisting of a quadrupole (Q) mass analyzer, a quadrupole collision cell, and a second-stage time-of-flight (TOF) analyzer. Positive ions were formed by using a needle voltage of 3 kV and a cone voltage of 90 V. The temperatures of the source block and for desolvation were 90 °C. A solution flow rate of 10 μL/min was used for introduction. All parameters (i.e., aperture to the TOF, transport voltage) were optimized to achieve maximum sensitivity and a mass resolving power of 10,000 (full width at half maximum). The spectra were a sum of 2-sec scans over 2 min, and the spectra were smoothed twice using a three-point Savitzky-Golay method before submitting the data to the Mathcad (MathSoft Engineering & Education Inc., Cambridge, MA) program for calculating the centroids.

Modeling

For kinetic modeling, the total number of active hydrogens (sites) was divided into three groups. The number of exchanging hydrogens in each group and the rate constant for each group were varied in a process that minimized the differences between the data and the model at various time-points. The deuterium uptake is the sum of number of exchangeable sites in each of the three groups. Deuterium uptake at each site was modeled as a pseudo first-order reaction to calculate the fraction of molecules that were deuterated at this site [15]. From this, the mass shift responsible for the shift of the mass centroid of the isotopic pattern was calculated.

The process for calculating the affinity constants

starts with the model for PLIMSTEX [23]. Specifically, the modeling of the mass change based on the solution concentrations was carried over from PLIMSTEX, but the equations for the oligomer solution concentrations were modified to accommodate self-association as described in [24]. To allow the program to find a reliable minimum and avoid being trapped in an unreasonable local minimum, the search was started at "good-guess" values. Good-guess values were obtained by synthesizing a model dataset on the basis of the start values, and then comparing the outcome to the experimental data. The initial good-guess values were modified until a good graphical fit was obtained. The "minimize" function in the program was then used to refine the sought-after solution by minimizing the square root of the mean of the squares of the differences between the data and the model over the concentration range of the titration. The minimization is a nonlinear, quasi-Newtonian method β_i and all the assumptions required for a NLLS regression are relevant [25].

The program started with guess values for the β_i involved in the association of insulin and the known total protein (ligand) concentration. The model was based on the reactions shown in eq 1.

$$\begin{aligned} &2Monomer \xrightarrow{K_{12}} Dimer \\ &2Dimer \xrightarrow{K_{24}} Tetramer \\ &Dimer + Tetramer \xrightarrow{K_{46}} Hexamer \end{aligned} \tag{1}$$

The unknown parameter β_i for the system were taken to be as those defined in eq 2

$$\begin{aligned} \beta_0 &= 1 \\ \beta_1 &= K_{12} \\ \beta_3 &= K_{24}K_{12}^2 \\ \beta_5 &= K_{46}K_{24}K_{12}^3 \end{aligned} \tag{2}$$

To give us consistent expressions for the following equations, β_2 and β_4 were set to zero. Using β_i to define the oligomer concentrations was more economical for the development of the equation. After solving for the β_i, individual affinity constants were obtained as shown in eq 3

$$\begin{aligned} K_{12} &= \beta_1 \\ K_{24} &= \frac{\beta_3}{\beta_1^2} \\ K_{46} &= \frac{\beta_5}{\beta_3\beta_1} \end{aligned} \tag{3}$$

Trial values for another model parameter, D_i, were also provided to the program; where D_i is the number of deuteriums protected in the i^{th} oligomer compared with that in the monomer. For example, D_0 is the number of amide hydrogens protected in the monomer and D_1 is the number protected in the dimer compared to the monomer, and so on.

The concentration of free ligand in solution was calculated by numerically integrating (using the "Rk-adapt") the function $\frac{d[Lig]}{d[Lig]_T}$, which was calculated as a reciprocal of the $\frac{d[Lig]_T}{d[Lig]}$, where [*Lig*] is the free ligand concentration in solution and $[Lig]_T$ is the total analytical concentration of the ligand as described in [23].

The mass shift caused by D uptake, ΔD, at any concentration during the titration was defined as the number of exchangeable sites in the molecule for each oligomer weighted by the corresponding fraction of monomers produced when the oligomer dissociates, subtracted from the number of exposed sites in the monomer. Equation 4 is the mathematical form of this description. Here N is 5.

$$\Delta D = f(Lig, \beta, D) = D_0 - \sum_{j=1}^{N} D_j \frac{(j+1)\beta_j Lig^j}{\sum_{i=0}^{N}(i+1)\beta_i Lig^i} \tag{4}$$

Each term in eq 4 contained a solution fraction arising from the oligomer before a common factor of [*Lig*] had been used to divide both the denominator and the numerator. The denominator is the total number of protein molecules from all oligomeric forms; that is, the number of molecules that would be detected in the mass spectrometer after quenching the amide exchange reaction. This method assumes that each constituent molecule has a characteristic number of exchangeable hydrogens. All the modeling and the plots were done in Mathcad 2001*i* (MathSoft, Inc., Cambridge, MA).

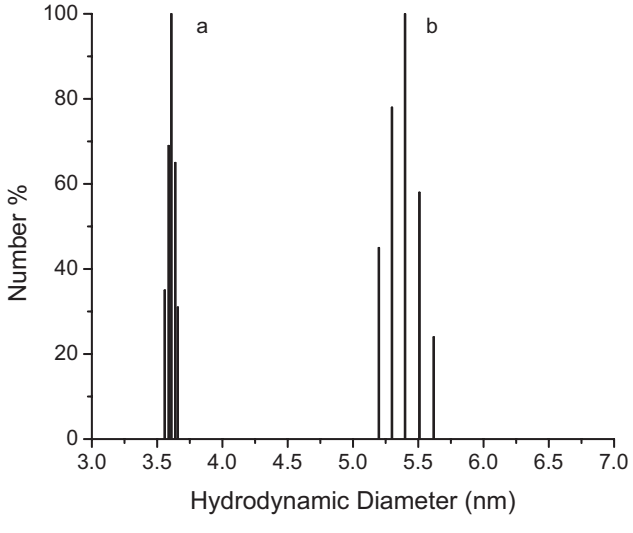

Figure 1. Overlay of hydrodynamic diameter distributions determined by DLS for human insulin at (**a**) pH 2.5. The mean diameter of the particles is 3.64 nm, suggesting a mixture of dimers and monomers in solution. (**b**) pH 7.4. The mean diameter of the particles is 5.43 nm, suggesting a mixture of higher oligomers.

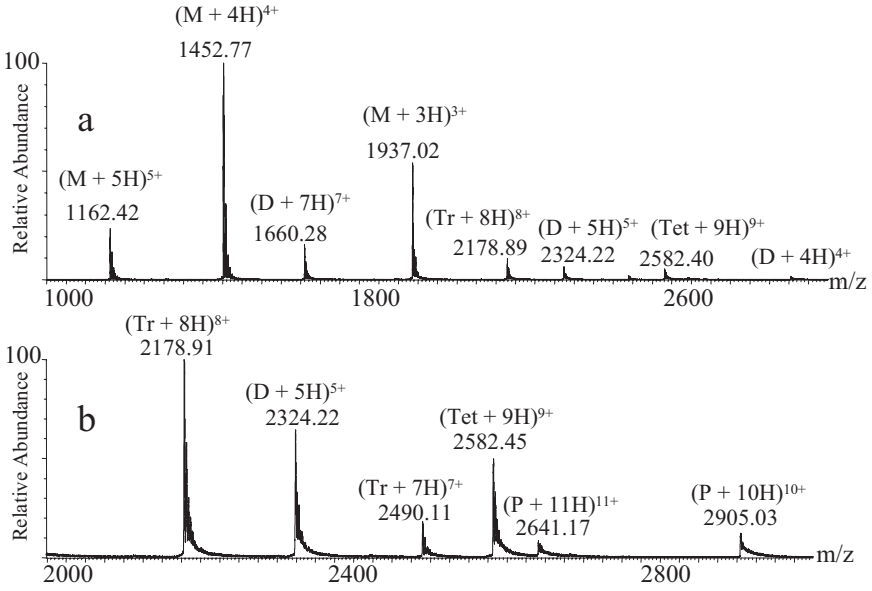

Figure 2. (**a**) Typical mass spectrum of r-human insulin sprayed from ammonium acetate (pH = 7.4). (**b**) Magnification of the region from 2000 to 3000 Da from (**a**) showing the multiply charged oligomers. The abbreviations used in the labeling are, D for dimer, Tr for trimer, Tet for tetramer, and P for pentamer.

Results and Discussion

Oligomers in the Gas Phase

The comparison of the molecular diameters obtained by DLS (Figure 1) with the values reported [26] reveals that insulin exists mainly as a mixture of monomers and dimers at pH 2.5; at pH 7.4, the mixture contains higher oligomers, mainly hexamers. To determine if ESI can introduce these oligomers into the gas-phase, we electrosprayed r-human insulin in ammonium acetate solution (pH = 7.4). The resulting mass spectrum (Figure 2) showed various oligomers of characteristic charge-state distributions, similar to the observation made by Robinson and coworkers [27] for bovine insulin. The resolving power of the Q-TOF did not permit us to distinguish the 8+ trimer from a 16+ hexamer. To obtain evidence for existence of oligomers in solution, we electrosprayed insulin solutions at different concentrations to determine whether a variation in the concentration of oligomers in solution produced a corresponding change in the oligomeric ions in the gas-phase. We found appreciable amount of oligomers in the mass spectrum only at the relatively high concentrations of 100 μM and 1 mM (data not shown) of total protein. The abundance of dimer in the spectrum is higher for the 1-mM solution, indicating that oligomerization increases with concentration. The high concentrations may be necessary to compensate for electrospray-induced dissociation of the oligomers, which are only held together by a few noncovalent interactions [2, 10, 11].

Investigating further, we electrosprayed lispro solutions from ammonium acetate at a pH of 7.4 (see Figure 3 for the monomer and dimer regions of the mass spectrum). We found that the abundance of lispro dimer in the gas phase was lower than that for r-human, suggesting that lispro self-associates to a lesser extent in

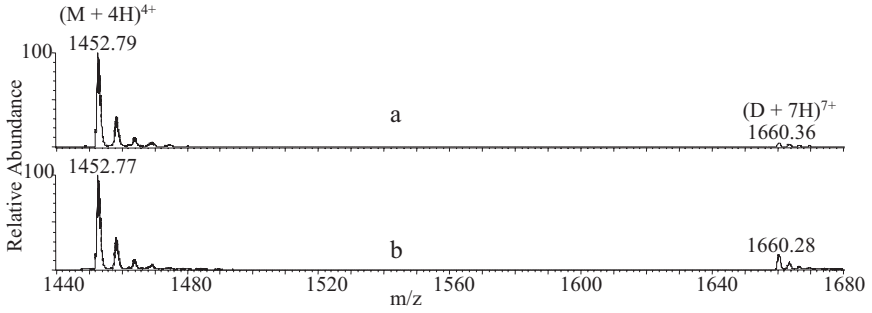

Figure 3. Monomer (4+) and dimer (7+) regions of (**a**) lispro, and (**b**) r-human insulins showing the difference in the oligomerization properties in solution. Monomer and dimer are represented by M and D, respectively.

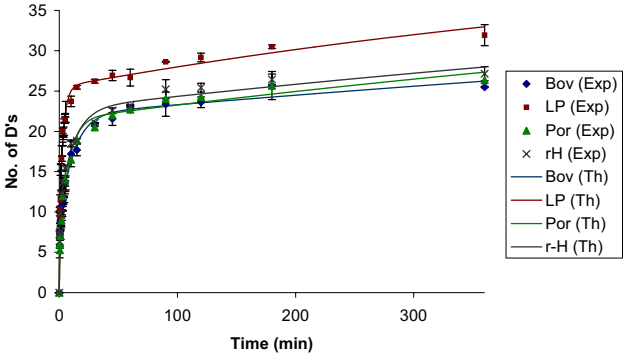

Figure 4. Time-dependent uptake of deuterium for various insulins in solution. The points are experimental data, and the solid curves are the best theoretical fit.

solution than r-human insulin. This agrees qualitatively with literature reports [9], indicating that ESI mass spectrometry can screen insulin analogs for self-association in solution.

The oligomerization models reported in literature [28], however, do not consider that a trimer or pentamer exists in solution. Nevertheless, they are seen in the gas phase of the mass spectrometer. We suggest that these gas-phase oligomers result from the dissociation of solution tetramers and hexamers during the process of ionization. Thus, the species seen in the gas phase may not reflect those in solution. To obtain a quantitative assessment of the oligomerization status of various insulin mutants in solution, we used H/D amide exchange experiments, the results from which are described below.

Kinetics of Amide Exchange in Solution

To obtain more information on the self-association and to differentiate better the oligomerization properties of various insulins, we followed the kinetics of amide H/D exchange by quenching the exchange at various times and monitoring the deuterium uptake by ESI MS. The H/D exchange was initiated by diluting a stock solution of insulin to the requisite concentration in a deuterated buffer. Dilution results in dissociation of higher oligomers (e.g., hexamers and tetramers), which are first-order kinetic processes. Insulin follows an EX2 mechanism of exchange as determined in 1968 [29]. On this basis, we assume that various steps in the reaction diagram follow an EX2 mechanism of exchange; exchange in which the rate-limiting step is the exchange of the exposed site.

The rates of exchange for all the insulins studied here reach a constant value in ~6 h (see Figure 4). Lispro insulin exchanges 32 deuterium atoms after 6 h, compared with 27 by r-human insulin, and reaches ~65% of steady-state value within 3 min after mixing, whereas r-human insulin reaches only 50% at that time. These comparisons reveal that lispro insulin is less self-associated than r-human insulin. Kinetic studies of H/D exchange for porcine and bovine insulins give similar results to those of r-human insulin. Although porcine insulin is most protected from exchange, the differences between r-human, bovine, and porcine insulins are small. These results are similar to the ones obtained earlier in this laboratory [14] under different solution conditions.

On the basis of earlier work with insulin [29] and our own work with calmodulin [15], we assume that kinetics for exchange can be classified in three groups: fast, intermediate, and slow. Applying the kinetic fit described in the Methods section allows us to obtain the number of hydrogens in each of the three groups (Table 3). Lispro has 21 slow hydrogens compared with 24 for r-human. Although more amide hydrogens of r-human insulin exchange more rapidly than those of lispro, there are more amides that exchange at intermediate rates for lispro. Some of the slow-exchanging amide hydrogens of r-human insulin exchange at intermediate rates for lispro, providing more evidence that lispro insulin is less self-associated in solution than is r-human insulin.

Similar to the results in [15], the number of hydrogens in the slow group for r-human increases with binding, indicating that binding protects amide hydrogens. This could occur either by burial of active hydrogens in the oligomer interface(s) or by changes in stability (H-bonding). Although the kinetics of exchange differentiate the self-association properties of various insulins, the difference between lispro and r-human is surprisingly small, given the large difference in the solution oligomerization properties. The kinetic properties of H/D amide exchange of the various oligomers in solution may not be well represented by the variation in the mass-centroid of the single insulin molecule whose mass we measure. Furthermore, it is not possible to partition the global kinetic effects among the various oligomers by doing an experiment at a single concentration. A titration experiment, similar to the one carried out in the PLIMSTEX [22] method, should be more informative.

Table 3. Number of amide hydrogens in the three kinetic groups for porcine, bovine, r-Human and lispro insulins

Insulin analog	No. of fast H's ($k_f > 3$ min^{-1})	No. of intermed. H's ($k_i \sim 0.2$ min^{-1})	No. of slow H's ($k_s \sim 0.001$ min^{-1})
Porcine	6 (± 1)	19 (± 0.5)	26 (± 0.5)
Bovine	10 (± 0.5)	16 (± 0.5)	25 (± 0.5)
r-Human	12 (± 1)	15 (± 0.5)	24 (± 0.5)
Lispro	9 (± 1)	21 (± 1)	21 (± 0.5)

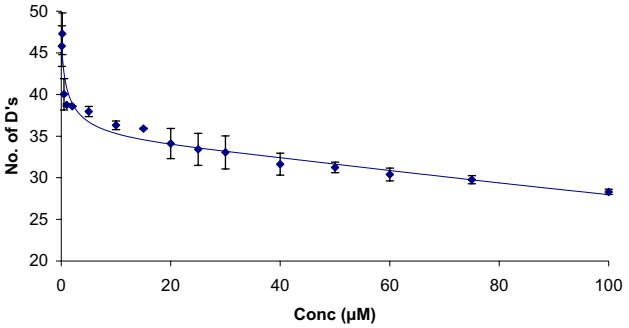

Figure 5. Plot of the uptake of deuterium as a function of solution concentration of r-human insulin. The points are the experimental data and the curves are the theoretical fit.

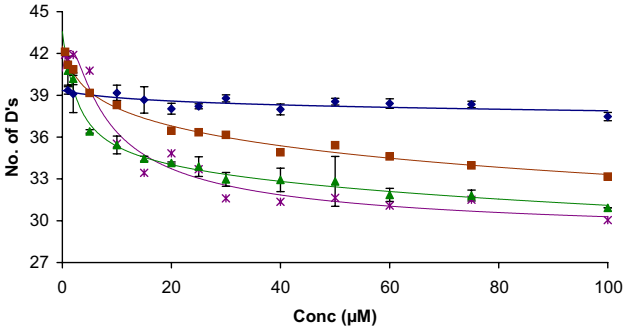

Figure 6. Plot of the extent of H/D exchange studied as a function of concentration for four insulin mutants. The points are the experimental data, and the solid curves are the theoretical fits to the data. The blue diamonds represent the data for lispro, the red squares for the mutant B13B21, the green triangles for the mutant B9Asp, and the purple asterisks for A4B27.

Self-Association Interactions by Mass Spectrometry, Self-Titration, and H/D Exchange (SIMSTEX)

Adapting PLIMSTEX for self-association requires first a measurement of deuterium uptake for monomeric insulin ions at steady-state exchange (e.g., 6 h as in Figure 4) as a function of the total insulin concentration. Second, the adaptation requires changes in modeling the titration curve to give the desired affinity constants. We call the adaptation of PLIMSTEX for the special case of self-association, SIMSTEX (see "Modeling" in the Methods section for a description of the changes).

We measured the deuterium uptake for r-human insulin at various concentrations after 6 h of exchange. The deuterium uptake for r-human insulin decreases gradually with increasing concentration of insulin (see the points in Figure 5). As the concentration increases, more oligomerization occurs, resulting in more amide hydrogens being protected. Fitting the experiment data with the SIMSTEX model gives, when the best fit is achieved, the theoretical curve in Figure 5.

As a starting point in applying SIMSTEX, we followed [28] the literature and assumed that the oligomerization of r-human insulin occurs by the process: monomer $\rightleftarrows$ dimer $\rightleftarrows$ tetramer $\rightleftarrows$ hexamer (i.e., $D \rightleftarrows T \rightleftarrows H$). A small value of $K24$ (see first row of data in Table 4) means that there is no significant tetramerization, leaving the most likely steps in oligomerization to be $D \rightleftarrows H$ (i.e., the reaction is monomer $\rightleftarrows$ dimer $\rightleftarrows$ hexamer) for r-human insulin. We then fit the data to a $D \rightleftarrows H$ model to obtain more accurate values for the affinity constants, as shown by the data in the row 2 of Table 4. The K_as calculated for the $D \rightleftarrows H$ model agree with literature values (from sedimentation equilibrium and CD) within a factor of 5 [30, 31]. The number of amides protected upon dimerization and hexamerization of r-human insulin are 18 and 25, respectively, compared with 51 exchangeable hydrogens in the monomer.

Application of SIMSTEX to Various Insulin Mutants

We studied lispro and the six insulin mutants shown in Table 2 by measuring the extent of H/D exchange for each as a function of their solution concentration (see Figure 6 for four of the mutants). Qualitatively, the deuterium uptakes and the shapes of the curves are indicators of the self-associating properties of the proteins. Insulin mutant, A4B27, for example, undergoes the least exchange at the highest concentration studied (100 μM), suggesting a high extent of self-association for this mutant in solution. Another mutant, B21, has the smallest initial slope for the six mutants, suggesting a low extent of dimerization. To obtain quantitative information on how these mutations affect the oligomerization properties, we applied SIMSTEX modeling.

The best fits to the data (see the curves in Figure 6) afford a set of oligomerization equilibrium constants (Table 5). We found that some of the mutations affect dimerization and hexamerization constants by as much

Table 4. Results from SIMSTEX modeling on r-human and lispro insulins. K_{12}, K_{24} and K_{26}/K_{46} are the dimerization, tetramerization and hexamerization constants, respectively, and the D_i values are number of deuterium protected in the i-th oligomer

Insulin analog	Model	K_{12} (M^{-1})	K_{24} (M^{-1})	K_{46} or K_{26}	D_2	D_4	D_6	D_0
r-Human	$D \rightleftarrows T \rightleftarrows H$	5×10^5	2×10^{-3}	3×10^{10} (M^{-1})	16	1	42	47
r-Human	$D \rightleftarrows H$	$7 \pm 2 \times 10^5$	–	$2 \pm 0.2 \times 10^9$ (M^{-2})	18 ± 3	–	25 ± 2	51 ± 1
r-Human (Lit.)		7.5×10^5 [30]		4×10^8 (M^{-2}) [31]				
		1.4×10^5 [31]						

Table 5. Oligomerization equilibrium constants for the six insulin mutants. The mutants were obtained by changing various residues in r-Human insulin, for which we determined $K_{12} = 7 \times 10^5$ (M^{-1}) and $K_{26} = 2 \times 10^9$ (M^{-2})

Insulin mutant	K_{12} (M^{-1})	K_{24} (M^{-1})	K_{26} or K_{46}
Lispro	$3 \pm 2 \times 10^4$	$3 \pm 2 \times 10^2$	–
A4A17	$2 \pm 2 \times 10^7$	–	$5.1 \pm 0.3 \times 10^{10}$ (M^{-2})
B27	–	$1 \pm 1 \times 10^{14}$	$3 \pm 3 \times 10^{11}$ (M^{-1})
A4B27	$2 \pm 1 \times 10^5$	$2.0 \pm 0.3 \times 10^5$	$2 \pm 1 \times 10^6$ (M^{-1})
B9Asp	$6 \pm 3 \times 10^4$	$8 \pm 1 \times 10^5$	$3 \pm 1 \times 10^4$ (M^{-1})
B21	$7 \pm 3 \times 10^3$	$2 \pm 2 \times 10^6$	–
B13B21	$5 \pm 1 \times 10^4$	$1 \pm 1 \times 10^7$	$3 \pm 2 \times 10^5$ (M^{-1})

as five orders of magnitude and that the effects vary from mutant to mutant.

We now consider the effect of each mutation and the agreement of the oligomerization equilibrium constants with literature reports. The exchange of lispro shows that a small initial decrease in exchange is quickly replaced by a nearly constant extent of exchange, suggesting either a cessation of the oligomerization or a formation of oligomers in which no additional amide hydrogens are protected. We obtained the affinity constants for lispro insulin by using a $D \rightleftarrows T$ model (row 1, Table 5). This choice of model became obvious when we found no appreciable hexamerization constant when using the $D \rightleftarrows T \rightleftarrows H$ model. The outcome shows that the equilibrium constant for lispro's dimerization agrees within a factor of twenty with that reported in literature [7]. This discrepancy is probably due to the small protection afforded upon dimerization (D_2 for lispro = 4; data not shown), giving rise to the nearly horizontal curve for lispro in Figure 6. SIMSTEX, similar to PLIMSTEX, requires that there be a change in the extent of H/D exchange upon binding for the method to work well. Accepting the values as estimates for the equilibrium constants, we see that lispro has a dimerization constant that is reduced by a factor of ~20 times compared to that of r-human insulin. Moreover, lispro does not hexamerize in the concentration range studied, further underscoring its lower tendency to form oligomers. The results are consistent with lispro being a faster-acting insulin than r-human, which is more persistent in vivo.

The equilibrium constants for dimerization and hexamerization of the insulin mutant A4A17 are not strongly affected by the mutations compared to those for human insulin (Table 5). We found a small effect on the equilibrium constants for the mutants A4 and A17, and this is consistent with the view that these residues are not involved in the dimerization or hexamerization. Furthermore, the mutant B27, an analog in which Thr at B27 is replaced by Arg, does not undergo any significant dimerization but, instead, forms a tetramer and a hexamer to a much higher extent than does human insulin. This insulin mutant has the property of prolonged action in vivo possibly because it has lower solubility (often precipitates at the site of injection into a human) and absorbs slowly [2, 3, 32]. The mutant A4B27 is more soluble, but its dimerization constant is five times less than that of r-human insulin. The equilibrium constant to give the hexamer is reduced by three orders of magnitude but that for formation of the tetramer is increased. These variations are possibly due to the change in pI caused by the replacement of Glu with Gln.

The three mutants, B9Asp, B21, and B13B21, have smaller equilibrium constants for hexamerization than does r-human insulin. The Asp at B9 (in place of a Ser) introduces a charge site in the B-chain and decreases self-association compared with that of r-human insulin [2, 3, 33, 34]. The replacement of Glu^{B21} to Gln causes such a significant decrease in self-association that no appreciable hexamer forms for B21. The mutation is in a β-turn that determines many of the secondary structural features of the insulin molecule [35]. The equilibrium constant for B13-B21 to give a hexamer is greater than that of B21, underscoring the role of Glu^{B13} in human insulin in promoting oligomerization. Replacement of Glu with Gln is known to decrease charge repulsion in the center of the hexamer and, thus, increase stability [13].

Conclusions

Application of SIMSTEX, a variant of PLIMSTEX, permits the determination of equilibrium constants for oligomerization of insulin and various insulin mutants. Changing amino acids B9, B13, B21, and B27 impact significantly the self-association of insulin. The mutant B13 forms hexamers more readily than r-human given the change of Glu to Gln, whereas mutants A4 and A17 undergo little oligomerization of this type, and mutant B9 (Ser to Asp) shows decreased tendency to self-associate. These results are in good agreement with those in the literature, motivating continued development and application of SIMSTEX not only for screening newly designed insulin analogs but also for studying self-association of larger proteins. Nevertheless, the results reveal a limitation of this approach, and of PLIMSTEX; that is, there must be for self-association, or binding, in general, a change in the number of amide hydrogens protected; evidence for this limitation is seen in the application of SIMSTEX to lispro.

There is also a serious question about this kinetic approach to equilibrium. Kinetics come into play in two steps of the experiment: first in the reorganization of the protein when its solution is diluted by adding D_2O to

start the exchange, and second in the actual kinetics of H/D exchange. How do the kinetics of these steps affect the SIMSTEX curves (and by analogy PLIMSTEX curves)? We currently assume in their application that the reorganization of the oligomer steady-state occurs rapidly when its solution is diluted with D_2O at the start of the exchange and that the H/D exchange follows an EX2 mechanism. Preliminary simulations in our laboratory show that the dissociation/association kinetics can distort the shape of the curve (i.e., the response that we observe as a mass shift versus insulin concentration). We find that the distortion is reduced to a level of no practical consequence for the determination of the oligomerization equilibrium constants if the H/D exchange kinetics are sufficiently slow compared with the dissociation/association kinetics. For insulin after 6 h of exchange, those exchange reactions involving amide hydrogens that exchange at fast and intermediate rates (Table 3) are essentially complete. This would leave only the amide hydrogens counted as slow in Table 3 to contribute to the changes in deuterium uptake as a function of insulin solution concentration shown in Figures 5 and 6. Simulation also suggests that the hydrogen–deuterium exchange rate constants of $\sim$0.001 min^{-1} and less are sufficiently small to produce minimal distortion in the SIMSTEX curves. The reasonable agreement of the equilibrium constants with those reported supports this conclusion, but future work is planned to examine these questions in more detail.

Acknowledgments

The authors thank FDA, St. Louis for providing the lispro, bovine, and porcine insulins, Karen Wooley of the Department of Chemistry for the use of the DLS instrument, and Stephen Bayne of NovoNordisk for the insulin mutants. Funding was provided by the National Center for Research Resources (NCRR) of the National Institutes of Health (grant no. 2P41RR00954).

References

1. Brange, J.; Langkjoer, L. Insulin Structure and Stability. *Pharm. Biotech.* **1993,** *5,* 315–350.
2. DeFelippis, M. R.; Chance, R. E.; Frank, B. H. Insulin Self-Association and the Relationship to Pharmacokinetics and Pharmacodynamics. *Crit. Rev. Therap. Drug. Carrier Sys.* **2001,** *18,* 201–264.
3. Brange, J.; Volund, A. Insulin Analogs with Improved Pharmacokinetic Profiles. *Adv. Drug Delivery Rev.* **1999,** *35,* 307–335.
4. Kang, S.; Brange, J.; Burch, A.; Volund, A.; Owens, D. R. Subcutaneous Insulin Absorption Explained by Insulin's Physicochemical Properties. Evidence from Absorption Studies of Soluble Human Insulin and Insulin Analogs in Humans. *Diabetes Care* **1991,** *14,* 942–948.
5. Holleman, F.; Hoekstra, J. B. L. Insulin Analogs: The Virtual Reality of Normal Insulin Secretion. *Nether. J. Med.* **1995,** *47,* 95–98.
6. Markussen, J.; Diers, I.; Engesgaard, A.; Hansen, M. T.; Hougaard, P.; Langkjaer, L.; Norris, K.; Ribel, U.; Soerensen, A. R. Soluble, Prolonged-Acting Insulin Derivatives. II. Degree of Protraction and Crystallizability of Insulins Substituted in Positions A17, B8, B13, B27, and B30. *Protein Eng.* **1987,** *1,* 215–223.
7. Brems, D. N.; Alter, L. A.; Beckage, M. J.; Chance, R. E.; DiMarchi, R. D.; Green, L. K.; Long, H. B.; Pekar, A. H.; Shields, J. E.; Frank, B. H. Altering the Association Properties of Insulin by Amino Acid Replacement. *Protein Eng.* **1992,** *5,* 527–533.
8. Pillai, O.; Panchagnula, R. Insulin Therapies—Past, Present, and Future. *Drug Discovery Today* **2001,** *6,* 1056–1061.
9. Holleman, F.; Hoekstra, J. B. L. Insulin Lispro. *N. Engl. J. Med.* **1997,** *337,* 176–183.
10. Blundell, T.; Dodson, G.; Hodgkin, D.; Mercola, D. Insulin Structure in the Crystal and Its Reflection in Chemistry and Biology. *Adv. Protein Chem.* **1972,** *26,* 279–402.
11. Baker, E. N.; Blundell, T. L.; Cutfield, J. F.; Cutfield, S. M.; Dodson, E. J.; Dodson, G. G.; Hodgkin, D. M.; Hubbard, R. E.; Isaacs, N. W.; Reynolds, C. D. The Structure of 2Zn Pig Insulin Crystals at 1.5 A Resolution. *Philosophical Transactions of the Royal Society of London* **1988,** *319,* 369–456.
12. Slieker, L. J.; Brooke, G. S.; DiMarchi, R. D.; Flora, D. B.; Green, L. K.; Hoffmann, J. A.; Long, H. B.; Fan, L.; Schields, J. E.; Sundell, K. L.; Surface, O. L.; Chance, R. E. Modifications in the B10 and B26-30 Regions of the B Chain of Human Insulin Alter Affinity for the Human IGF-I Receptor More than for the Insulin Receptor. *Diabetologia* **1997,** *40,* S54–S61.
13. Bentley, G. A.; Brange, J.; Derewenda, Z.; Dodson, E. J.; Dodson, G. G.; Markussen, J.; Wilkinson, A. J.; Wollmer, A.; Xiao, B. Role of B13 Glu in Insulin Assembly. The Hexamer Structure of Recombinant Mutant (B13 Glu - > Gln) Insulin. *J. Mol. Biol.* **1992,** *228,* 1163–1176.
14. Ramanathan, R.; Gross, M. L.; Zielinski, W. L.; Layloff, T. P. Monitoring Recombinant Protein Drugs: A Study of Insulin by H/D Exchange and Electrospray Ionization Mass Spectrometry. *Anal. Chem.* **1997,** *69,* 5142–5145.
15. Zhu, M. M.; Rempel, D. L.; Zhao, J.; Giblin, D. E.; Gross, M. L. Probing Ca2+ Induced Conformational Changes in Porcine Calmodulin by H/D Exchange and ESI-MS: Effect of Cations and Ionic Strength. *Biochemistry* **2003,** *42,* 15388–15397.
16. Zhang, Z.; Smith, D. L. Determination of Amide Hydrogen Exchange by Mass Spectrometry: A New Tool for Protein Structure Elucidation. *Protein Sci.* **1993,** *2,* 522–531.
17. Engen, J. R.; Smith, D. L. Investigating Protein Structure and Dynamics by Hydrogen Exchange MS. *Anal. Chem.* **2001,** *73,* 256A–265A.
18. Eyles, S. J.; Gumerov, D. R.; Gierasch, L. M.; Kaltashov, I. A. Probing Protein Folding and Binding by Electrospray Ionization Fourier Transform Mass Spectrometry. *Adv. Mass Spectrom.* **2001,** *15,* 499–500.
19. Mandell, J. G.; Baerga-Ortiz, A.; Akashi, S.; Takio, K.; Komives, E. A. Solvent Accessibility of the Thrombin–Thrombomodulin Interface. *J. Mol. Biol.* **2001,** *306,* 575–589.
20. Komives, E. A. Protein–Protein Interaction Dynamics by Amide H/H-2 Exchange Mass Spectrometry. *Int. J. Mass Spectrom.* **2005,** *240,* 285–290.
21. Powell, K. D.; Ghaemmaghami, S.; Wang, M. Z.; Ma, L.; Oas, T. G.; Fitzgerald, M. C. A General Mass Spectrometry-Based Assay for the Quantitation of Protein–Ligand Binding Interactions in Solution. *J. Am. Chem. Soc.* **2002,** *124,* 10256–10257.
22. Zhu, M. M.; Rempel, D. L.; Du, Z.; Gross, M. L. Quantification of Protein–Ligand Interactions by Mass Spectrometry, Titration, and H/D Exchange: PLIMSTEX. *J. Am. Chem. Soc.* **2003,** *125,* 5252–5253.
23. Zhu, M. M.; Rempel, D. L.; Gross, M. L. Modeling Data from Titration, Amide H/D Exchange, and Mass Spectrometry to Obtain Protein-Ligand Binding Constants. *J. Am. Soc. Mass Spectrom.* **2004,** *15,* 388–397.
24. Chitta, R. K.; Rempel, D. L.; Gross, M. L. Determination of Affinity Constants and Response Factors of the Noncovalent Dimer of Gramicidin by Electrospray Ionization Mass Spectrometry and Mathematical Modeling. *J. Am. Soc. Mass Spectrom.* **2005,** *16,* 1031–1038.
25. Johnson, M. L. Why, When, and How Biochemists Should Use Least Squares. *Anal. Biochem.* **1992,** *206,* 215–225.
26. Kadima, W.; Oegendal, L.; Bauer, R.; Kaarsholm, N.; Brodersen, K.; Hansen, J. F.; Porting, P. The Influence of Ionic Strength and pH on the Aggregation Properties of Zinc-Free Insulin Studied by Static and Dynamic Laser Light Scattering. *Biopolymers* **1993,** *33,* 1643–1657.
27. Nettleton, E. J.; Tito, P.; Sunde, M.; Bouchard, M.; Dobson, C. M.; Robinson, C. V. Characterization of the Oligomeric States of Insulin in Self-Assembly and Amyloid Fibril Formation by Mass Spectrometry. *Biophys. J.* **2000,** *79,* 1053–1065.
28. Pocker, Y.; Biswas, S. B. Self-Association of Insulin and the Role of Hydrophobic Bonding: A Thermodynamic Model of Insulin Dimerization. *Biochemistry* **1981,** *20,* 4354–4361.
29. Praissman, M.; Rupley, J. A. Comparison of Protein Structure in the Crystal and in Solution. II. Tritium-Hydrogen Exchange of Zinc-Free and Zinc Insulin. *Biochemistry* **1968,** *7,* 2431–2445.
30. Pekar, A. H.; Frank, B. H. Conformation of Proinsulin. Comparison of Insulin and Proinsulin Self-Association at Neutral pH. *Biochemistry* **1972,** *11,* 4013–4016.
31. Holladay, L. A.; Ascoli, M.; Puett, D. Conformational Stability and Self-Association of Zinc-Free Bovine Insulin at Neutral pH. *Biochim. Biophys. Acta.* **1977,** *494,* 245–254.
32. Markussen, J.; Diers, I.; Hougaard, P.; Langkjaer, L.; Norris, K.; Snel, L.; Soerensen, A. R.; Soerensen, E.; Voigt, H. O. Soluble, Prolonged-Acting Insulin Derivatives. II. Degree of Protraction, Crystallizability, and Chemical Stability of Insulins Substituted in Positions A21, B13, B23, B27, and B30. *Protein Eng.* **1988,** *2,* 157–166.
33. Volund, A.; Brange, J.; Drejer, K.; Jensen, I.; Markussen, J.; Ribel, U.; Sorensen, A. R.; Schlichtkrull, J. In Vitro and in Vivo Potency of Insulin Analogs Designed for Clinical Use. *Diabetic Med.* **1991,** *8,* 839–847.
34. Jorgensen, A. M.; Kristensen, S. M.; Led, J. J.; Balschmidt, P. Three-Dimensional Solution Structure of an Insulin Dimer. A Study of the B9(Asp) Mutant of Human Insulin Using Nuclear Magnetic Resonance, Distance Geometry, and Restrained Molecular Dynamics. *J. Mol. Biol.* **1992,** *227,* 1146–1163.
35. Wang, S. H.; Hu, S. Q.; Burke, G. T.; Katsoyannis, P. G. Insulin Analogs with Modifications in the β-Turn of the B-chain. *J. Protein Chem.* **1991,** *10,* 313–324.